EXACT SENSITIVITY ANALYSIS AND OPTIMIZATION FOR MULTI-COUPLED MICROWAVE COMMUNICATION FILTERS

J.W. Bandler, S.H. Chen and S. Daijavad

SOS-84-16-R

September 1984

EXACT SENSITIVITY ANALYSIS AND OPTIMIZATION FOR MULTI-CAVITY MICROWAVE COMMUNICATION FILTERS

J.W. Bandler, S.H. Chen and S. Daijavad

Simulation Optimization Systems Research Laboratory and

Department of Electrical and Computer Engineering

McMaster University, Hamilton, Canada L8S 4L7

Tel. 416-525-9140 Ext. 4305

Summary

The development of modern communication systems demands frequent application of multi-coupled cavity filters. The theory originated by Atia and Williams [1] has inspired many advances in this area. The increasing variety and complexity of the design and manufacture of these filters necessitate the employment of modern computer-aided design techniques. We have developed a systematic and efficient approach to the simulation and exact sensitivity evaluation of multi-coupled cavity filters. The network parameters as well as non-ideal effects such as losses are treated directly as possible variables. Both first- and second-order derivatives, including exact group delay and its sensitivities, are considered. Arbitrary terminations and filter structures can be easily accommodated. The usefulness of the approach presented here is highlighted by selected examples of very practical applications.

A narrow-band lumped model of an unterminated multi-cavity filter has been given by Atia and Williams [1] as

$$\mathrm{j}\,\mathbf{Z}\mathbf{I} = \mathbf{V}\ , \tag{1}$$

where

$$\mathbf{Z} \triangleq (s\,\mathbf{1} + \mathbf{M}) \ , \tag{2}$$

1 denotes an nxn identity matrix and **M** the nxn coupling matrix whose (i, j) element represents the normalized coupling between the ith and jth cavities and the diagonal entries M_{ii} represent the deviations from synchronous tuning. The normalized frequency variable s in (2) is given by

$$s \triangleq \frac{\omega_0}{\Delta\omega}\left(\frac{\omega}{\omega_0} - \frac{\omega_0}{\omega}\right), \tag{3}$$

where ω_0 is the synchronously tuned cavity resonant frequency and $\Delta\omega$ is the bandwidth parameter.

The system can be reduced to a two-port model whose parameters and sensitivity expressions can be obtained by solving the real systems

$$\mathbf{Zp} = \mathbf{e}_1 \ , \tag{4}$$

$$\mathbf{Zq} = \mathbf{e}_n \ , \tag{5}$$

$$\mathbf{Z}\bar{\mathbf{p}} = \mathbf{p} \tag{6}$$

and

$$\mathbf{Z}\bar{\mathbf{q}} = \mathbf{q} \ , \tag{7}$$

where $\mathbf{e}_1 \triangleq [1\ 0\ 0\ \ldots\ 0]^T$ and $\mathbf{e}_n \triangleq [0\ 0\ \ldots\ 0\ 1]^T$. The solutions of (4) - (7) require only one real LU factorization of matrix **Z**. The two-port model, including the input and output transformers, is given by

$$\begin{bmatrix} I_1 \\ I_n \end{bmatrix} = -j\,\mathbf{y}\begin{bmatrix} V_1 \\ V_n \end{bmatrix} = -j\begin{bmatrix} y_{11} & y_{12} \\ y_{21} & y_{22} \end{bmatrix}\begin{bmatrix} V_1 \\ V_n \end{bmatrix}, \tag{8}$$

where

$$\mathbf{y} = \begin{bmatrix} y_{11} & y_{12} \\ y_{21} & y_{22} \end{bmatrix} = \begin{bmatrix} n_1^2 p_1 & n_1 n_2 p_n \\ n_1 n_2 p_n & n_2^2 q_n \end{bmatrix}, \tag{9}$$

n_1 and n_2 being the input and output transformer ratios, respectively. Utilizing the solutions of (4) - (7), first-order and second-order sensitivity expressions of **y** have been derived. Special features of the network model such as the lossless property and the possible anti-symmetry of the coupling matrix have been exploited in order to optimize the computational efficiency.

Detailed results are available [2]. Some typical results are selected and shown in Table 1. Full results will be presented at the symposium.

The input and output currents of the filter terminated by a load Z_L and a normalized voltage source E = 1V with an impedance Z_S can be solved to be

$$\mathbf{I}_p = \begin{bmatrix} I_1 \\ \\ I_n \end{bmatrix} = -j\,\hat{\mathbf{Y}}^{-1}\mathbf{y}\,\mathbf{e}_1, \tag{10}$$

where

$$\hat{\mathbf{Y}} \triangleq \mathbf{1} - j\,\mathbf{y}\,\hat{\mathbf{Z}} \tag{11}$$

and

$$\hat{\mathbf{Z}} \triangleq \begin{bmatrix} Z_S & 0 \\ 0 & Z_L \end{bmatrix}. \tag{12}$$

The sensitivities of $\mathbf{I}_p$ are given by

$$\frac{\partial \mathbf{I}_p}{\partial \phi} = j\,\hat{\mathbf{Y}}^{-1}\,\frac{\partial \mathbf{y}}{\partial \phi}\,[\hat{\mathbf{Z}}\,\mathbf{I}_p - \mathbf{e}_1], \tag{13}$$

$$\frac{\partial \mathbf{I}_p}{\partial \omega} = j\,\hat{\mathbf{Y}}^{-1}\left[\left(\frac{\partial \mathbf{y}}{\partial \omega}\,\hat{\mathbf{Z}} + \mathbf{y}\frac{\partial \hat{\mathbf{Z}}}{\partial \omega}\right)\mathbf{I}_p - \frac{\partial \mathbf{y}}{\partial \omega}\mathbf{e}_1\right] \tag{14}$$

and

$$\frac{\partial^2 \mathbf{I}_p}{\partial \phi \partial \omega} = j\,\hat{\mathbf{Y}}^{-1}\left[\left(\frac{\partial^2 \mathbf{y}}{\partial \phi \partial \omega}\,\hat{\mathbf{Z}} + \frac{\partial \mathbf{y}}{\partial \phi}\,\frac{\partial \hat{\mathbf{Z}}}{\partial \omega}\right)\mathbf{I}_p + \frac{\partial \mathbf{y}}{\partial \phi}\,\hat{\mathbf{Z}}\,\frac{\partial \mathbf{I}_p}{\partial \omega} + \left(\frac{\partial \mathbf{y}}{\partial \omega}\,\hat{\mathbf{Z}} + \mathbf{y}\frac{\partial \hat{\mathbf{Z}}}{\partial \omega}\right)\frac{\partial \mathbf{I}_p}{\partial \phi} - \frac{\partial^2 \mathbf{y}}{\partial \phi \partial \omega}\mathbf{e}_1\right]. \tag{15}$$

From these results, various filter responses and their sensitivities are readily formulated. For example, denoting the insertion loss by Δ, we have

$$\frac{\partial \Delta}{\partial \phi} = \frac{-20}{\ell n 10}\,\mathrm{Re}\left[\frac{1}{I_n}\,\frac{\partial I_n}{\partial \phi} + \frac{1}{Z_L + Z_S}\left(\frac{\partial Z_L}{\partial \phi} + \frac{\partial Z_S}{\partial \phi}\right)\right]. \tag{16}$$

The group delay and its sensitivity w.r.t. $M_{\ell k}$ can be computed by

$$T_G = -\mathrm{Im}\left[\frac{1}{I_n}\,\frac{\partial I_n}{\partial \omega} + \frac{1}{Z_L}\,\frac{\partial Z_L}{\partial \omega}\right] \tag{17}$$

and

$$\frac{\partial T_G}{\partial M_{\ell k}} = -\,\mathrm{Im}\left[\frac{1}{I_n}\,\frac{\partial^2 I_n}{\partial M_{\ell k}\,\partial \omega} - \frac{1}{I_n^2}\,\frac{\partial I_n}{\partial M_{\ell k}}\,\frac{\partial I_n}{\partial \omega}\right], \tag{18}$$

respectively. Explicit formulas for other filter responses of engineering interest such as the input and output reflection coefficients and the gain slope have also been derived [2].

The computational efficiency and flexibility of our approach have made the application of modern CAD techniques to many engineering problems possible and very practical. In conjunction with a powerful, exact-gradient-based minimax method [3], our approach has been implemented in a computer program to produce optimal filter designs. Network parameters such as the coupling values are solved directly.

Self-equalized filters satisfying stringent specifications on both amplitude and phase responses are of great interest to the design of satellite communication systems. Figure 1 shows the responses of a nonminimum-phase filter resulting from simultaneous optimization of amplitude and group delay. Based upon a nominal design obtained by using an ideal model, the behaviour of the actual devices can be predicted by taking the non-ideal effects into account using appropriate sensitivity information.

Figure 2 shows the predicted non-ideal response of a 6-pole filter assuming uniform cavity dissipations.

The correct identification of parameters deviating from nominal design provides essential information for automatic tuning of manufactured filters. One such example of a 10-th order filter, employing the ℓ_1 optimization technique for identification [4], is illustrated in Figs. 3 and 4. Our approach, with the capacity of accommodating arbitrary terminations, can also be efficiently incorporated with the simulation and optimization of a large network into which the filters may be embedded, such as a multiplexer. The external network can be appropriately modelled as equivalent terminations.

References

[1] A.E. Atia and A.E. Williams, "New types of waveguide bandpass filters for satellite transponders", COMSAT Technical Review, vol. 1, 1971, pp. 21-43.

[2] J.W. Bandler, S.H. Chen and S. Daijavad, "Efficient approaches to the simulation of narrow-band multi-cavity filters", Department of Electrical and Computer Engineering, McMaster University, Hamilton, Canada, Report SOS-84-9-R, 1984.

[3] J. Hald and K. Madsen, "Combined LP and quasi-Newton methods for minimax optimization", Mathematical Programming, vol. 20, 1981, pp. 49-62.

[4] J. Hald and K. Madsen, "Combined LP and quasi-Newton methods for nonlinear ℓ_1 optimization", SIAM J. on Numerical Analysis, to be published.

TABLE 1

SELECTED SENSITIVITY EXPRESSIONS

Variable	Derivative	Sensitivity Expressions
$\Phi = M_{\ell k}$	$\frac{\partial y}{\partial M_{\ell k}}$ †	$C_1 \begin{bmatrix} 2n_1^2 p_\ell p_k & n_1 n_2 (p_\ell q_k + p_k q_\ell) \\ n_1 n_2 (p_\ell q_k + p_k q_\ell) & 2n_2^2 q_\ell q_k \end{bmatrix}$
$\Phi = \omega, \Delta\omega, \omega_0$	$\frac{\partial y}{\partial \Phi}$	$-\frac{\partial s}{\partial \Phi} \begin{bmatrix} n_1^2 \mathbf{p}^T \mathbf{p} & n_1 n_2 \mathbf{q}^T \mathbf{p} \\ n_1 n_2 \mathbf{q}^T \mathbf{p} & n_2^2 \mathbf{q}^T \mathbf{q} \end{bmatrix}$
$\Phi = r_i$ ††	$\frac{\partial y}{\partial r_i}$	$j \begin{bmatrix} n_1^2 p_i^2 & n_1 n_2 p_i q_i \\ n_1 n_2 p_i q_i & n_2^2 q_i^2 \end{bmatrix}$
$\Phi = M_{\ell k}$	$\frac{\partial^2 y}{\partial M_{\ell k} \partial \omega}$ †††	$C_2 \begin{bmatrix} 2n_1^2 (p_\ell \bar{p}_k + p_k \bar{p}_\ell) & n_1 n_2 (p_\ell \bar{q}_k + p_k \bar{q}_\ell + \bar{p}_\ell q_k + \bar{p}_k q_\ell) \\ n_1 n_2 (p_\ell \bar{q}_k + p_k \bar{q}_\ell + \bar{p}_\ell q_k + \bar{p}_k q_\ell) & 2n_2^2 (q_\ell \bar{q}_k + q_k \bar{q}_\ell) \end{bmatrix}$

† where $C_1 \triangleq \begin{cases} -\frac{1}{2} & \text{if } \ell = k \\ -1 & \text{otherwise} \end{cases}$

†† r_i is the lumped resistive parameter of the ith cavity.

††† $C_2 \triangleq \begin{cases} \frac{1}{2} \frac{\partial s}{\partial \omega} & \text{if } \ell = k \\ \frac{\partial s}{\partial \omega} & \text{otherwise} \end{cases}$

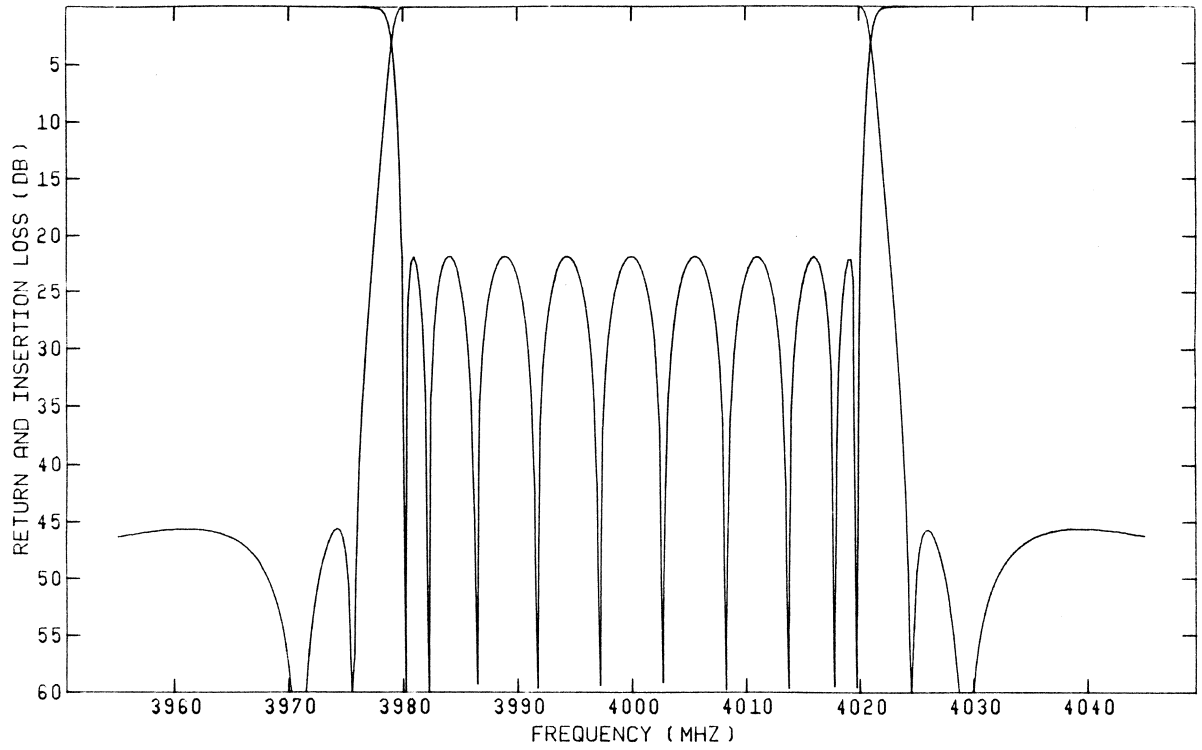

(a) Return loss and insertion loss response.

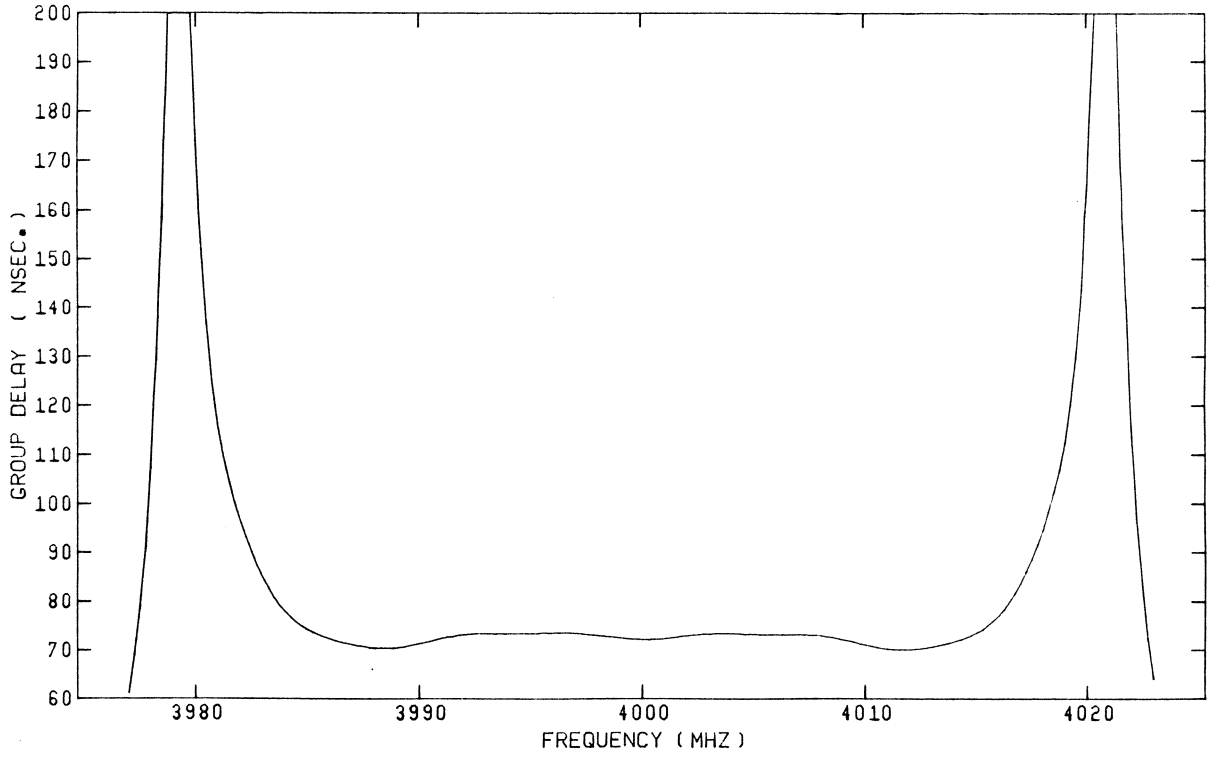

(b) Group delay response.

Fig. 1 Responses of the synchronously tuned 10-pole filter showing optimized amplitude and group delay.

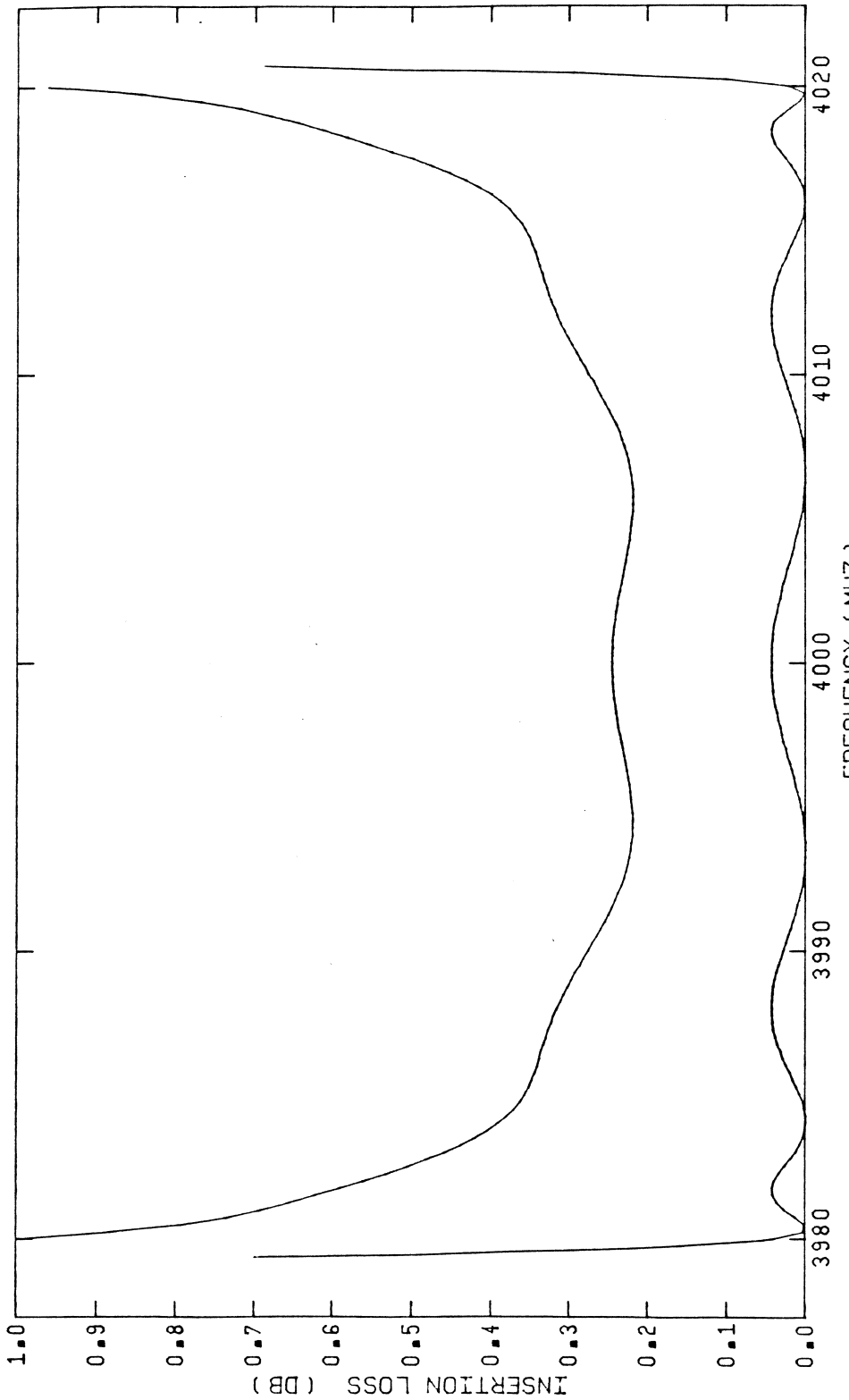

Fig. 2 Predicted response of a 6-pole filter assuming uniform cavity dissipations. Unloaded $Q = 12000$. The result is indistinguishable from the exact simulation of the lossy filter.

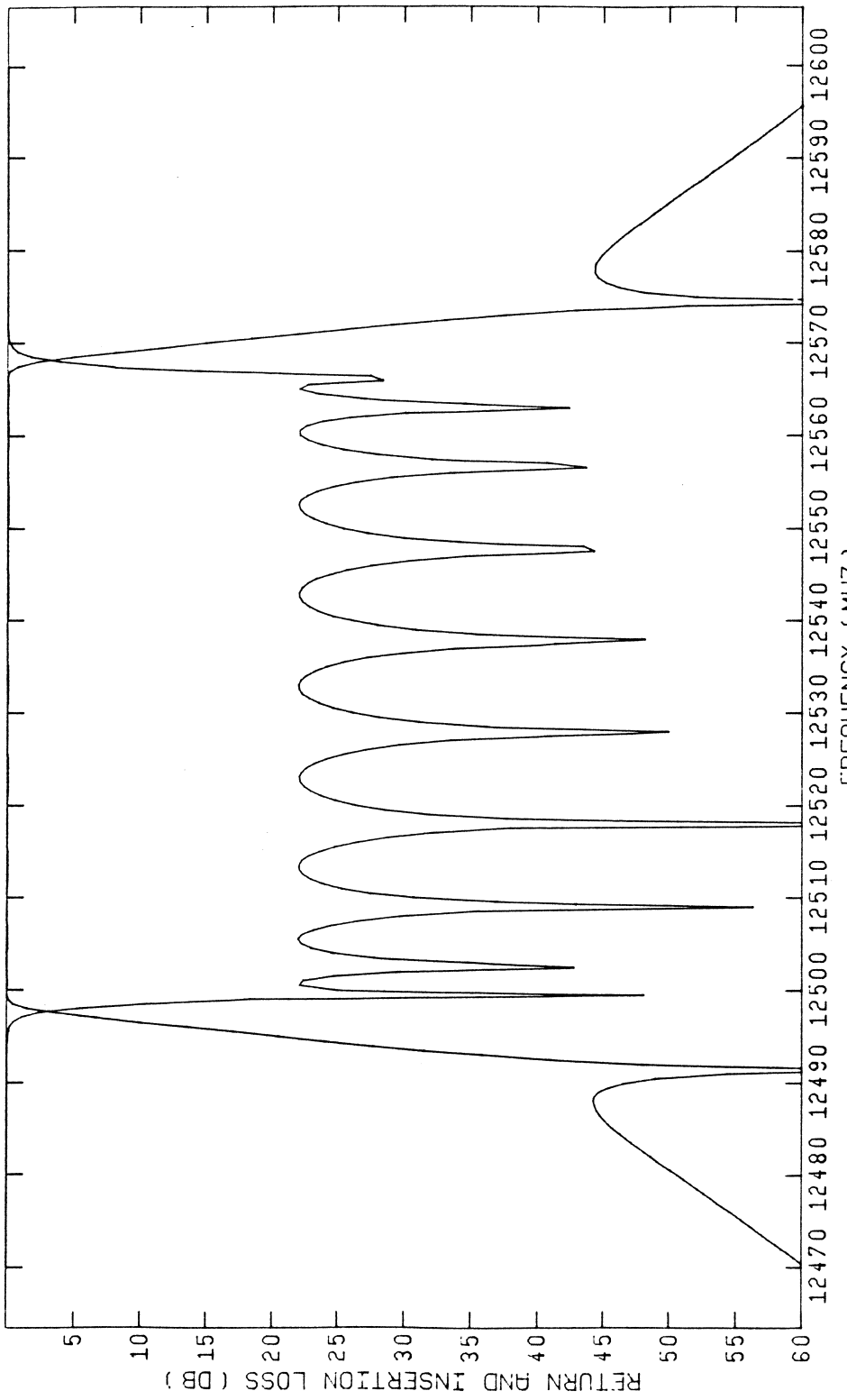

Fig. 3 Return and insertion loss responses of an optimally designed 10th order filter.

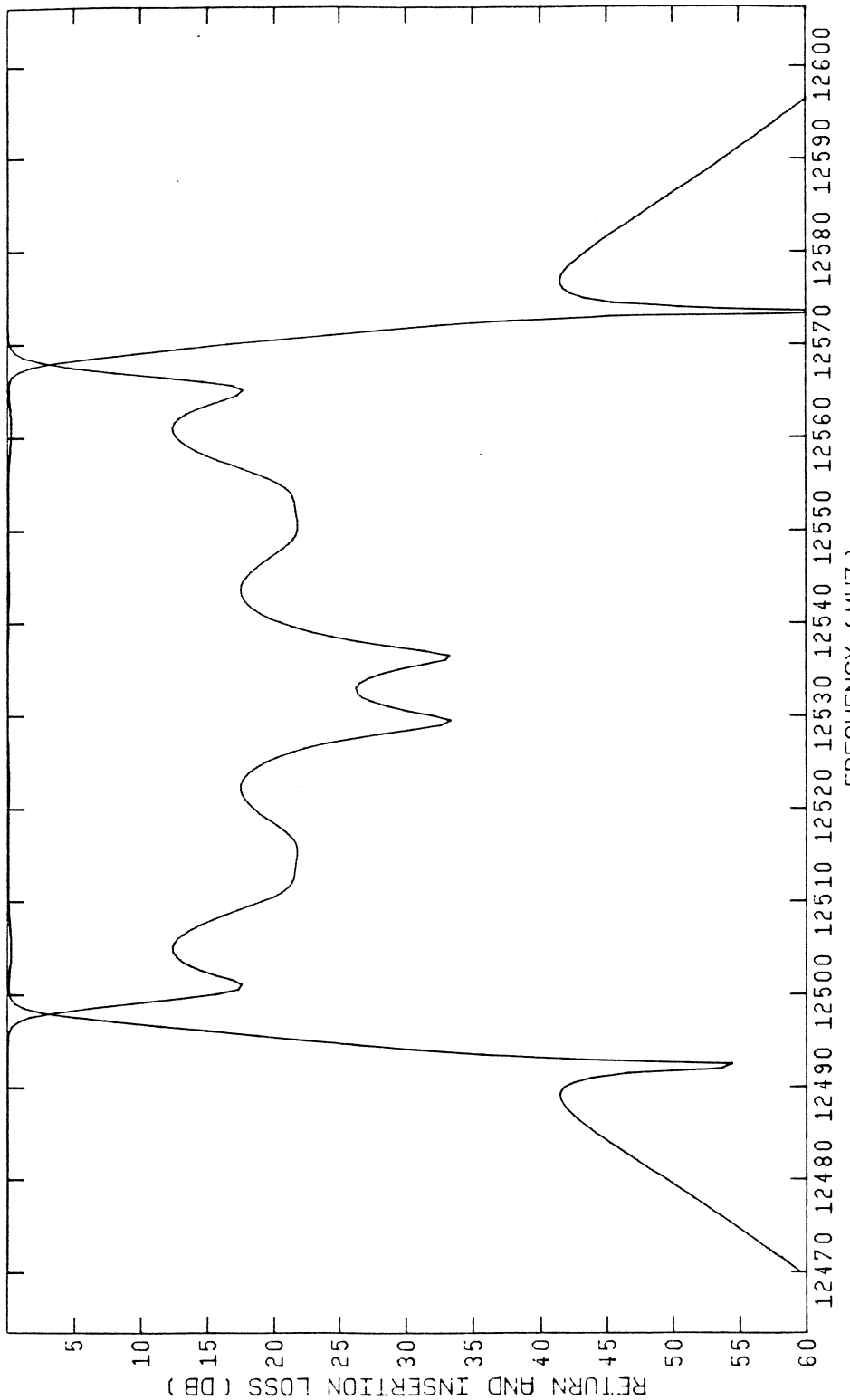

Fig. 4 Return and insertion loss responses of the 10th order filter after perturbation of some ideal parameters. The perturbed parameters are successfully identified and the response after the identification is indistinguishable from the original perturbed response.